Journal of Applied Geodesy 5 (2011), 99–115 © de Gruyter 2011. DOI 10.1515/JAG.2011.010

An optimal sensor fusion method for skew-redundant inertial measurement units

Yigiter Yuksel and Naser El-Sheimy

Abstract. To achieve the required navigation accuracy in some navigation applications, it is necessary to use a number of inertial sensors to obtain higher-quality acceleration/rotation rate measurements. For such redundant units, an inertial sensor fusion algorithm is required. This algorithm optimally combines all sensor outputs and generates a single inertial measurement that may be processed by any existing navigation software. In this study, a comprehensive framework for the inertial sensor fusion problem is presented for the skew-redundant inertial measurement units. An optimal sensor fusion algorithm is then developed for the skew-redundant units, where all of the inertial sensors are arbitrarily oriented in space without any lever-arm effect. An error model for the algorithm output is also derived, and it is shown that under certain conditions, the number of states for these error models can be greatly reduced. Simulation test results show that when inertial sensors with complimentary characteristics are used, the proposed fusion algorithm can be used to form high-accuracy inertial measurements, which inherit all the best characteristics of the constituent sensors in the skew-redundant units.

Keywords. Inertial navigation, redundant IMU, sensor fusion.

1. Introduction

There are some navigation applications (e.g., pipeline mapping, self-guided autonomous vehicles) for which the performance of current microelectromechanical system (MEMS) inertial units are not sufficient to achieve required navigation accuracies. For such applications, one of the foreseeable solutions is to use a redundant number of inertial sensors together (as the size and power constraints permit) to obtain more accurate navigation data.

Redundant sensor configurations have been used in inertial navigation applications for a very long time (Evans and Wilcox 1970). However, until recently, the use of redundant systems has been strictly confined only to the fault detection and isolation (FDI) problem. As it is reviewed in the next section, the existing FDI methods deal with the reliability of the systems, which has no direct relation to the problem of improving navigation accuracy. This is the point at which this study deviates from the existing literature. In this study, sensor redundancy is used for the sole purpose of obtaining better acceleration and rotation rate measurements from a skew-redundant inertial measurement unit (SRIMU). Therefore, nothing has been proposed or claimed about the fault tolerance in this article. The objective of this study is to define (compute) the best acceleration and rotation rate that can be obtained from an SRIMU.

In the vast majority of the existing literature, a simple weighted average of the healthy sensor outputs of an SRIMU is used to run the navigation algorithms. In the next section, a conceptual example is presented to show why this study seeks to define another solution. In Section 4.1, the optimal solution of this example will also be presented.

1.1. A conceptual example

Let us assume that we have a rotating wheel fixed around its center. The objective is to compute the total rotation of this wheel using 2 gyroscopes placed on the wheel. It is assumed that these 2 gyroscopes have the following output models:

$$\underbrace{\begin{bmatrix} y_k^1 \\ y_k^2 \end{bmatrix}}_{\mathbf{y}_k} = \underbrace{\begin{bmatrix} 1 \\ 1 \end{bmatrix}}_{\mathbf{M}} \omega_k + \underbrace{\begin{bmatrix} x_k^1 \\ 0 \end{bmatrix}}_{\mathbf{x}_k} + \underbrace{\begin{bmatrix} 0 \\ v_k^2 \end{bmatrix}}_{\mathbf{v}_k} \tag{1a}$$

where y_k^1 and y_k^2 are raw outputs of the two gyroscopes whose sensitive axis are parallel to the axis of the wheel, ω_k is the true rotation rate of the wheel, v_k^2 is the additive white noise on the gyroscope 2, and x_k^1 is the stability error of the gyroscope 1, which is modeled as a random walk process as shown in the following:

$$x_{k+1}^1 = x_k^1 + w_k^1 \tag{1b}$$

$$E\left\{ \begin{bmatrix} x_0^1 \\ w_k^1 \\ v_k^2 \\ 1 \end{bmatrix} \begin{bmatrix} x_0^1 \\ w_k^1 \\ v_l^2 \end{bmatrix}^T \right\} = \begin{bmatrix} P_0 & 0 & 0 \\ 0 & Q_k\delta_{kl} & 0 \\ 0 & 0 & R_k^1\delta_{kl} \\ 0 & 0 & 0 \end{bmatrix}. \tag{1c}$$

The rotation angle of the wheel can be represented in discrete time as follows:

$$x^a_{k+1} = x^a_k + \Delta t \omega_k$$
$$x^a_0 = 0 \tag{2}$$

where x^a_k is the total rotation angle of the wheel, Δt is the discretization time, and ω_k is he rotation rate as described in equation (1a).

The objective is to compute a single rotation rate estimate from the two gyroscopes, so that the rotation angle in equation (2) can be computed. For this aim, one can propose several policies, three of which are described here.

i. Policy I

Directly inspired by the existing studies on FDI, the following solution can be proposed to define a combined rotation rate measurement:

$$\hat{\omega}_k = (\mathbf{M}^T \mathbf{R}_k^{-1} \mathbf{M})^{-1} \mathbf{M}^T \mathbf{R}_k^{-1} \mathbf{y}_k \tag{3a}$$

where $\mathbf{R}_k = E\{\mathbf{v}_k \mathbf{v}_k^T\}$ and $\mathbf{M}$ is defined in equation (1). Although $\mathbf{R}_k$ is not invertible according to (1a), equation (3a) can be written in the limiting sense as:

$$\hat{\omega}_k = y^1_k \tag{3b}$$

As seen from equation (3b), this policy completely ignores the second gyroscope.

ii. Policy II

If one prefers to use both of the sensors, an arbitrary weight matrix $\mathbf{W}_k$ can be used in equation (3a) instead of $\mathbf{R}_k$. However, in this case the selection of $\mathbf{W}_k$ becomes extremely important because a poor selection would cause worse results than would Policy I.

iii. Policy III

This policy uses the following method to compute a rotation rate estimate:

$$\hat{\omega}_k = y^1_k - \frac{1}{(k+1)} \sum_{i=0}^{k} (y^1_k - y^2_k). \tag{4}$$

If the stability error of gyroscope 1 (x^1_k) has a relatively small disturbance power (i.e., $Q_k \approx 0$), this policy can effectively eliminate the initial bias error (initial uncertainty of the stability error) of the gyroscope 1. Therefore, this policy can provide accurate rotation rate measurements under such conditions.

As seen from this conceptual example, given a redundant measurement unit, one can come up with many different policies to compute a single, combined acceleration/rotation rate measurement. It is obvious that some of these policies are better than the others. This leads to the following questions:

i. How can an optimal solution to this problem be defined?
ii. How can such an optimal solution be computed?

This paper aims to answer these simple, yet essential questions while defining an optimal sensor fusion algorithm for the SRIMUs.

1.2. Review of the existing literature

The redundant inertial sensor configurations are used for the sole purpose of FDI in the vast majority of the existing literature. The initial examples of such redundant systems can be found in the studies of Evans and Wilcox (1970), Bejczy (1971), Wilcox (1973), Pejsa (1974), and Harrison et al. (1977). These initial studies mostly analyze the sensor configurations that provide better FDI. Sturza (1988) generalizes such efforts on redundant configurations based on two different criteria. In the work of Sukkarieh (2000), the same problem is handled in the context of information filters. However, in all of these studies, the so-called optimum configurations are determined under the assumption that the additive white noise is the only source of the sensor errors. Such an assumption cannot be presumed to be valid for low-cost MEMS units whose output error characteristics are usually dominated by other factors (Yuksel 2010). Therefore, it would be wrong to assume that the suggested conic (polyhedral) configurations can still be considered optimal for the MEMS-based SRIMUs.

In general, any FDI method consists of two basic steps (Patton et al. 2000, Frank 1990, Basseville 1996). The first step is residual generation. In this step, a measurement (residual) is formed using sensor outputs. These residuals are then processed by a detection algorithm to check for any faults in the second step. Several detection algorithms have been proposed in the literature: Evans and Wilcox (1970) used voting schema; Daly et al. (1979) described a generalized likelihood test; DeAngelis (1990) proposed a min-max type method that aims to minimize worst-case performance; Chen and Adams (1976) used sequential probability likelihood ratio tests; Ray (1989) utilized sequential tests that use a moving window of observation for decision. Finally, an extensive review of these methods (and many other variations) can be found in the works of Ho (1999) and Kerr (1987).

Basically, two methods are used for redundant inertial systems to generate residuals. The first method is the parity vector (Wilcox 1973, Desai and Ray 1981, Skoogh and Lennartsson 2006). In this method, the residuals are generated as the projection of observations to the left null space of the configuration matrix. In Chow and Willsky's study (1984), this parity approach is extended to cover analytical redundancy methods that were first described by Deckert et al. (1977). The second residual generation method is the compensated parity vector method (Hall 1982). In the surveys of Frank (1990) and Patton and Ghent (1994), the same method is named as the dedicated observer approach, and some additional examples based on Luenberger observers as well as Kalman filters are presented.

In the compensated parity approach, a Kalman filter is used to whiten the parity vectors, which eventually become a zero mean signal independent of the (actuator) inputs. The innovation process of the Kalman filter, which is driven by the parity vectors, is then used as the so-called compensated residuals in the decision algorithms. In this approach, all sensor errors are modeled in the Kalman filter. Therefore, in the course of whitening the parity vectors, these sensor errors are also implicitly estimated. However, these estimated variables are never used to correct the sensor outputs in the FDI methods because such a policy can cause complete failure of the system in case of any missed detection. In all of the studies listed earlier, the final combined output is generated as some form of weighted combination of healthy sensor outputs (Ho 1999). Despite the vast amount of FDI-oriented studies, only a very limited number of papers propose to use SRIMUs to improve the overall accuracy. In the study of Bar-Itzhack and Harman (2002), gyroscope quadruplet outputs are processed in a Kalman filter to self-calibrate the SRIMU errors. However, the proposed method requires a dynamical model for the rotation rates. Some combinations of the raw sensor outputs are used as an observation for the navigation Kalman filters in the work of Jia (2004). However, the basis for the selection of such combinations is not described. In the entire literature, Pittelkau (2005a, 2005b, 2006) was the first to provide a systematic treatment of the use of redundant sensors for the sole purpose of navigation accuracy enhancement. In these studies, it was proposed that the inertial navigation system (INS) should be run with a weighted average of the SRIMU outputs and that the sensor's parity vectors must be used as observations in the navigation Kalman filter. However, the optimality of such a solution is not defined at all in these studies. The reason that the navigation equations are executed with the average IMU outputs is defined as a practical solution to avoid the use of dynamical models of the space vehicle, as suggested by Bar-Itzhack and Harman (2002). Although this seems like a very natural approach for the SRIMU-based INSs, such an intuitive approach cannot be used to define the optimality of the combined sensor outputs.

As can be seen from this review, the existing literature falls short of presenting a compact theoretical treatment for an optimal sensor fusion algorithm. Although the fault detection studies stand on a very strong theoretical foundation, they simply ignore any question regarding the optimal sensor fusion problem. On the other hand, the remaining studies do not deal with a proper definition for the optimality of the intuitive selections, which are mainly inspired by the FDI methods. One of the purposes of this study is to fill this gap in the existing literature.

1.3. Scope and content of this study

In this study, an optimal sensor fusion algorithm for SRIMUs is derived. The context and the constraints of this study follow:

1. The sensor fusion problem is defined as the estimation of best acceleration/rotation rates on the body frame given a redundant number of inertial sensor outputs. The use of external navigation aids (such as GPS) is not considered a part of the fusion problem.
2. It is assumed that all of the sensors in the SRIMU are placed at the same point in space (no lever-arm effect is considered)
3. It is assumed that the configuration (orientation) of the sensors is predefined. This study does not deal with the redundant sensor configuration problem at all. As described in the previous section, the so-called optimum configurations cannot be assumed optimal for the low-cost MEMS units. Furthermore, such configurations are not practical by any means when tens of sensors are used in a SRIMU. Therefore, in this study, all the derivations are based on a predefined, yet arbitrary, sensor configuration. It is also essential to note that the optimality claim is hence limited to this predefined configuration.
4. It is assumed that the sensors in the SRIMU are perfectly calibrated. Although the calibration

errors can always be handled as a part of the sensor errors, this requires an intermediate calibration parameterization step that is not discussed in this study (such examples can be found in the work of Allerton and Jia (2002).

5. This study does not investigate the relation between specific sensor error components and the overall accuracy of the system. It is assumed that all sensor errors are modeled as Markov processes. Therefore, all simulations are performed assuming generic Markov process parameters without establishing any link between the parameters and their physical meanings.
6. In this study, the objective is limited to the estimation of best sensor output, rather than obtaining the best navigation solution. In general, the navigation solutions that are generated by running an INS with optimally fused sensor outputs are not the optimal navigation solutions (this point will be illustrated in Section 4.1). Although the optimal navigation solution problem uses exactly the same theoretical framework described in this study, this problem is not explicitly discussed in the context of this study.

2. Theoretical foundation of the proposed solution

In this section, the theoretical foundation of the proposed solution will be derived based on an abstract system definition. The association of this abstract system definition with the SRIMUs will be explained in the next section.

2.1. *Problem formulation and cost function definition*

Let us assume that a system is characterized by the following dynamical system representation.

$$\mathbf{x}_{k+1} = \mathbf{A}_k\mathbf{x}_k + \mathbf{N}_k\mathbf{u}_k + \mathbf{B}_k\mathbf{w}_k \tag{5a}$$

$$\mathbf{y}_k = \mathbf{C}_k\mathbf{x}_k + \mathbf{M}_k\mathbf{u}_k + \mathbf{v}_k \tag{5b}$$

$$E\left\{\begin{bmatrix}\mathbf{x}_0\\ \mathbf{w}_k\\ \mathbf{v}_k\end{bmatrix}\begin{bmatrix}\mathbf{x}_0\\ \mathbf{w}_l\\ \mathbf{v}_l\\ \mathbf{I}\end{bmatrix}^T\right\} = \begin{bmatrix}\mathbf{P}_0 & \mathbf{0} & \mathbf{0} & \mathbf{0}\\ \mathbf{0} & \mathbf{Q}_k\delta_{kl} & \mathbf{0} & \mathbf{0}\\ \mathbf{0} & \mathbf{0} & \mathbf{R}_k\delta_{kl} & \mathbf{0}\end{bmatrix}, \quad \forall k,l \tag{6}$$

where $\mathbf{x}_k$ is the state vector of the system with an initial covariance $\mathbf{P}_0$, $\mathbf{u}_k$ is the input vector that is assumed to be a deterministic unknown, and $\mathbf{y}_k$ represents the observations. $\mathbf{w}_k$ and $\mathbf{v}_k$ denote white system disturbance and observation noises with covariance matrices $\mathbf{Q}_k$ and $\mathbf{R}_k$. In this study, $\mathbf{M}_k$ is called a configuration matrix, which is assumed to have full column rank. $\mathbf{A}_k$, $\mathbf{N}_k$, $\mathbf{B}_k$, and $\mathbf{C}_k$ are matrices with appropriate dimensions.

In the context of SRIMUs, $\mathbf{y}_k$ represents the entire SRIMU outputs (measured acceleration/rotation rates), $\mathbf{u}_k$ is the real acceleration/rotation rate that the SRIMU is expected to measure, and $\mathbf{x}_k$ is the inertial sensor error vector (e.g., sensors' repeatability and stability errors). On the other hand, in the rest of this section, the derivations will be based only on equation (5) without referring any such physical meanings. A detailed association of equation (5) to SRIMUs will be presented in Section 3.

Under this general system definition, the objective is to causally estimate $\mathbf{x}_n$ and $\mathbf{u}_n$, given $\{\mathbf{y}_k\}_{k=0}^{n}$ $\forall k$. This causality condition implies that this study only deals with the filtering solution.

In this study, the following cost function is used to derive an optimal solution of this estimation problem:

$$\min_{\mathbf{x}_0,\mathbf{w}_k,\mathbf{u}_k} \|\mathbf{x}_0\|^2_{\mathbf{P}_0^{-1}} + \sum_{k=0}^{n-1}\|\mathbf{w}_k\|^2_{\mathbf{Q}_k^{-1}} + \sum_{k=0}^{n}\|\mathbf{y}_k - \mathbf{C}_k\mathbf{x}_k - \mathbf{M}_k\mathbf{u}_k\|^2_{\mathbf{R}_k^{-1}} \tag{7a}$$

Subject to

$$\mathbf{x}_{k+1} = \mathbf{A}_k\mathbf{x}_k + \mathbf{N}_k\mathbf{u}_k + \mathbf{B}_k\mathbf{w}_k \tag{7b}$$

where $\|\ \|^2_{\bullet}$ notation defines (squared) weighted L2 norm (i.e., $\|x\|^2_Y = x^T Yx$).

The $\{\mathbf{x}_n, \mathbf{u}_n\}$ pair that minimizes equation (7) is defined as the best (optimal) solution at time n. The selection of this cost function was motivated for the following reasons:

1. $\mathbf{u}_k$ in equation (5) does not have any stochastic descriptor (i.e., it is a deterministic unknown). Although the standard minimum mean square estimation methods (e.g., Kalman filtering) can also be used to define a solution for such mixed random/nonrandom problems, they require limit operations for the derivations.
2. Equation (7) is a deterministic cost function. Therefore, the weight matrices (i.e., $\mathbf{P}_0$, $\mathbf{Q}_k$, $\mathbf{R}_k$), do not have to represent any stochastic value. This property is especially important for MEMS

sensors for which modeling errors theoretically invalidate the optimality of the Kalman filters.

3. When all of the stochastic variables are assumed to have Gaussian distribution, equation (7) corresponds to the logarithm of density function $\mathrm{pdf}(\mathbf{y}_0 \ldots \mathbf{y}_n, \mathbf{x}_0, \mathbf{w}_0 \ldots \mathbf{w}_{n-1}; \mathbf{u}_0 \ldots \mathbf{u}_n)$. Therefore, under these conditions, the optimum solution of equation (7) also becomes optimum in the sense of minimum mean square and maximum likelihood.

In the following section, an algorithm to solve this deterministic cost function is described.

2.2. *Solution of the quadratic cost function optimization*

In this section, a filtering algorithm is derived for the optimal $\mathbf{x}_n$ and $\mathbf{u}_n$ solution of the quadratic optimization problem defined in equation (7).

The proposed solution to this optimization problem depends on the results presented by Hassibi (et al. 1999, Chapter 3). For the sake of completeness, the relevant result of Hassibi et al. (1999) is summarized in the following:

Lemma 1

Let a deterministic optimization problem be defined as follows:

$$\min_{\mathbf{x}_0, \mathbf{w}_k} \|\mathbf{x}_0\|^2_{\mathbf{P}_0^{-1}} + \sum_{k=0}^{n-1} \|\mathbf{w}_k\|^2_{\mathbf{Q}_k^{-1}} + \sum_{k=0}^{n} \|\mathbf{y}_k - \mathbf{C}_k\mathbf{x}_k\|^2_{\mathbf{R}_k^{-1}} \tag{8a}$$

Subject to

$$\mathbf{x}_{k+1} = \mathbf{A}_k\mathbf{x}_k + \mathbf{B}_k\mathbf{w}_k \tag{8b}$$

At time n, the optimal value of $\mathbf{x}_n$, which minimizes equation (8), is equivalent to the optimal $\hat{\mathbf{x}}_{n|n}$ result of the Kalman filter ($\mathbf{x}_n$ estimate given in all of the observations up to and including $\mathbf{y}_n$), defined for the following system:

$$\begin{aligned} \mathbf{x}_{k+1} &= \mathbf{A}_k\mathbf{x}_k + \mathbf{B}_k\mathbf{w}_k \\ \mathbf{y}_k &= \mathbf{C}_k\mathbf{x}_k + \mathbf{v}_k \end{aligned} \tag{9a}$$

$$E\left\{ \begin{bmatrix} \mathbf{x}_0 \\ \mathbf{w}_k \\ \mathbf{v}_k \\ 1 \end{bmatrix} \begin{bmatrix} \mathbf{x}_0 \\ \mathbf{w}_k \\ \mathbf{v}_k \end{bmatrix}^T \right\} = \begin{bmatrix} \mathbf{P}_0 & \mathbf{0} & \mathbf{0} \\ \mathbf{0} & \mathbf{Q}_k & \mathbf{0} \\ \mathbf{0} & \mathbf{0} & \mathbf{R_k} \\ \mathbf{0} & \mathbf{0} & \mathbf{0} \end{bmatrix}, \quad \forall k. \tag{9b}$$

For the proof, see the work of Hassibi et al. (1999, Lemma 3.2.1, 3.2.3, and 3.3.1). Unfortunately, Lemma 1 cannot be directly used to obtain the optimal solution of equation (7) because of the extra term $\mathbf{u}_k$ in equation (7). Therefore, using a series of linear transformations and change of variables, equation (7) must be converted into a form for which Lemma 1 can be applied. Once such a form is obtained, the Kalman filter described in Lemma 1 can be used to compute the solution for the optimization problem. The remaining part of this section mainly explains these required transformations.

First of all, using two successive linear transformations, equation (5b) is divided into two sets of observations as described in the following:

Let $\hat{\mathbf{T}}_k = \begin{bmatrix} \mathbf{T}_k \\ \overline{\mathbf{T}}_k \end{bmatrix}$ be a nonsingular square matrix, such that rows of $\mathbf{T}_k$ represent the basis vectors of the left null space of $\mathbf{M}_k$ and the rows of $\overline{\mathbf{T}}_k$ are the orthogonal complement of the rows of $\mathbf{T}_k$. In other words,

$$\mathbf{T}_k\mathbf{M}_k = \mathbf{0} \tag{10a}$$

$$\mathrm{Range}\{\overline{\mathbf{T}}_k^T\} = \mathrm{Range}\{\mathbf{M}_k\}. \tag{10b}$$

After the multiplication of $\hat{\mathbf{T}}_k$ with observation $\mathbf{y}_k$ in equation (5b), the following two sets of observations are obtained:

$$\mathbf{y}_k^1 = \mathbf{T}_k\mathbf{y}_k = \mathbf{T}_k\mathbf{C}_k\mathbf{x}_k + \mathbf{T}_k\mathbf{v}_k \tag{11a}$$

$$\mathbf{y}_k^2 = \overline{\mathbf{T}}_k\mathbf{y}_k = \overline{\mathbf{T}}_k\mathbf{C}_k\mathbf{x}_k + \overline{\mathbf{T}}_k\mathbf{M}_k\mathbf{u}_k + \overline{\mathbf{T}}_k\mathbf{v}_k. \tag{11b}$$

Furthermore, using the LDU decomposition of $\hat{\mathbf{T}}_k\mathbf{R}_k\hat{\mathbf{T}}_k^T$ (where $\mathbf{R}_k = E\{\mathbf{v}\mathbf{v}_k^T\}$), a second transformation is defined as follows:

$$\mathbf{V}_k = \begin{bmatrix} \mathbf{I} & \mathbf{0} \\ \underbrace{-\overline{\mathbf{T}}_k\mathbf{R}_k\mathbf{T}_k^{\mathbf{T}}(\mathbf{T}_k\mathbf{R}_k\mathbf{T}_k^T)^{-1}}_{-\tilde{\mathbf{T}}_k} & \mathbf{I} \end{bmatrix}. \tag{12}$$

The observations in equation (11) are transformed once more using $\mathbf{V}_k$:

$$\mathbf{y}_k^1 = \mathbf{T}_k\mathbf{y}_k = \mathbf{T}_k\mathbf{C}_k\mathbf{X}_k + \overbrace{\mathbf{T}_k\mathbf{v}_k}^{\mathbf{v}_k^1} \tag{13a}$$

$$\mathbf{y}_k^3 = \mathbf{y}_k^2 - \tilde{\mathbf{T}}_k\mathbf{y}_k^1 = \underbrace{(\overline{\mathbf{T}}_k - \tilde{\mathbf{T}}_k\mathbf{T}_k)}_{\mathbf{T}_k^3}\mathbf{C}_k\mathbf{x}_k + \underbrace{\overline{\mathbf{T}}_k\mathbf{M}_k}_{\mathbf{M}_k^3}\mathbf{u}_k + \underbrace{(\overline{\mathbf{T}}_k - \tilde{\mathbf{T}}_k\mathbf{T}_k)\mathbf{v}_k}_{\mathbf{v}_k^3}. \tag{13b}$$

It should be noted that $\mathbf{M}_k^3$ is a nonsingular matrix. Furthermore, due to the second transformation, $\mathbf{v}_k^1$ and $\mathbf{v}_k^3$ are orthogonal:

$$E\left\{\begin{bmatrix}\mathbf{v}_k^1\\ \mathbf{v}_k^1\end{bmatrix}\begin{bmatrix}\mathbf{v}_k^1\\ \mathbf{v}_k^1\end{bmatrix}^T\right\}=\begin{bmatrix}\mathbf{T}_k\mathbf{R}_k\mathbf{T}_k^T & \mathbf{0}\\ \mathbf{0} & \overline{\mathbf{T}}_k\mathbf{R}_k\overline{\mathbf{T}}_k^T-\overline{\mathbf{T}}_k\mathbf{R}_k\mathbf{T}_k^T(\mathbf{T}_k\mathbf{R}_k\mathbf{T}_k^T)^{-\mathbf{1}}\mathbf{T}_k\mathbf{R}_k\overline{\mathbf{T}}_k^T\end{bmatrix}\triangleq\begin{bmatrix}\mathbf{R}_k^1 & \mathbf{0}\\ \mathbf{0} & \mathbf{R}_k^3\end{bmatrix}. \tag{14}$$

Because of this orthogonality property, the cost function in equation (7) can be rewritten in terms of the final transformed observations as follows:

$$\min_{\mathbf{x}_0,\mathbf{w}_k,\mathbf{u}_k}\left(\|\mathbf{x}_0\|^2_{\mathbf{P}_0^{-1}}+\sum_{k=0}^{n-1}\|\mathbf{w}_k\|^2_{Q_k^{-1}}+\sum_{k=0}^{n}\|\mathbf{y}_k^1-\mathbf{T}_k\mathbf{C}_k\mathbf{x}_k\|^2_{(\mathbf{R}_k^1)^{-1}}+\sum_{k=0}^{n}\|\mathbf{y}_k^3-\mathbf{T}_k^3\mathbf{C}_k\mathbf{x}_k-\mathbf{M}_k^3\mathbf{u}_k\|^2_{(\mathbf{R}_k^3)^{-1}}\right) \tag{15a}$$

Subject to

$$\mathbf{x}_{k+1}=\mathbf{A}_k\mathbf{x}_k+\mathbf{N}_k\mathbf{u}_k+\mathbf{B}_k\mathbf{w}_k \tag{15b}$$

Now, the following change of variable is applied on equation (15):

$$\mathbf{z}_k=\mathbf{y}_k^3-\mathbf{T}_k^3\mathbf{C}_k\mathbf{x}_k-\mathbf{M}_k^3\mathbf{u}_k. \tag{16}$$

After this variable change, equation (15) can be written as:

$$\min_{\mathbf{x}_k,\mathbf{w}_k,\mathbf{z}_k}\left(\|\mathbf{x}_0\|^2_{\mathbf{P}_0^{-1}}+\sum_{k=0}^{n-1}\|\mathbf{w}_k\|^2_{\mathbf{Q}_k^{-1}}+\sum_{k=0}^{n}\|\mathbf{y}_k^1-\mathbf{T}_k\mathbf{C}_k\mathbf{x}_k\|^2_{(\mathbf{R}_k^1)^{-1}}+\sum_{k=0}^{n}\|\mathbf{z}_k\|^2_{(\mathbf{R}_k^3)^{-1}}\right) \tag{17a}$$

Subject to

$$\begin{aligned}\mathbf{x}_{k+1}&=\mathbf{A}_k\mathbf{x}_k+\mathbf{N}_k((\mathbf{M}_k^3)^{-\mathbf{1}}(\mathbf{y}_k^3-\mathbf{T}_k^3\mathbf{C}_k\mathbf{x}_k-\mathbf{z}_k))+\mathbf{B}_k\mathbf{w}_k\\&=(\mathbf{A}_k-\mathbf{N}_k(\mathbf{M}_k^3)^{-\mathbf{1}}\mathbf{T}_k^3\mathbf{C}_k)\mathbf{x}_k+\mathbf{B}_k\mathbf{w}_k-\mathbf{N}_k(\mathbf{M}_k^3)^{-\mathbf{1}}\mathbf{z}_k+\mathbf{N}_k(\mathbf{M}_k^3)^{-\mathbf{1}}\mathbf{T}_k^3\mathbf{y}_k\end{aligned} \tag{17b}$$

To get rid of the deterministic input $\mathbf{y}_k$ from constraints equation (17b), the following dynamical change of variables is introduced:

Let $\mathbf{x}_k=\mathbf{x}_k^e+\mathbf{x}_k^N$ and $\mathbf{y}_k^1=\mathbf{y}_k^e+\mathbf{y}_k^N$, where $\mathbf{x}_k^N$ and $\mathbf{y}_k^N$ is defined as

$$\mathbf{x}_{k+1}^N=(\mathbf{A}_k-\mathbf{N}_k(\mathbf{M}_k^3)^{-\mathbf{1}}\mathbf{T}_k^3\mathbf{C}_k)\mathbf{x}_k^N+\mathbf{N}_k(\mathbf{M}_k^3)^{-\mathbf{1}}\mathbf{T}_k^3\mathbf{y}_k \tag{18a}$$

$$\mathbf{y}_k^N=\mathbf{T}_k\mathbf{C}_k\mathbf{x}_k^N \tag{18b}$$

$$\mathbf{x}_0^N=0. \tag{18c}$$

Replacing $\mathbf{x}_k$ and $\mathbf{y}_k^1$ in equation (17) with $\mathbf{x}_k^e+\mathbf{x}_k^N$ and $\mathbf{y}_k^e+\mathbf{y}_k^N$, the following equivalent cost function is obtained:

$$\min_{\mathbf{x}_0^e,\mathbf{w}_k,\mathbf{z}_k}\left(\|\mathbf{x}_0^e\|^2_{\mathbf{P}_0^{-1}}+\sum_{k=0}^{n-1}\|\mathbf{w}_k\|^2_{\mathbf{Q}_k^{-1}}+\sum_{k=0}^{n}\|\mathbf{y}_k^e-\mathbf{T}_k\mathbf{C}_k\mathbf{x}_k^e\|^2_{(\mathbf{R}_k^1)^{-1}}+\sum_{k=0}^{n}\|\mathbf{z}_k\|^2_{(\mathbf{R}_k^3)^{-1}}\right) \tag{19a}$$

Subject to

$$\mathbf{x}_{k+1}^e=(\mathbf{A}_k-\mathbf{N}_k(\mathbf{M}_k^3)^{-\mathbf{1}}\mathbf{T}_k^3\mathbf{C}_k)\mathbf{x}_k^e+\mathbf{B}_k\mathbf{w}_k-\mathbf{N}_k(\mathbf{M}_k^3)^{-\mathbf{1}}\mathbf{z}_k \tag{19b}$$

The final form given in equation (19) is equivalent to the form defined in Lemma 1. Therefore, Lemma 1 can now be used directly to find the optimal solution for this quadratic cost function. Once the optimal solution of equation (19) is computed, the optimal solution of equation (7) can be obtained by simply reversing the change of variable operations. These results are summarized in Lemma 2.

Lemma 2

i. The optimal $\hat{\mathbf{x}}_n^e$ solution for the cost defined in equation (19) is equal to the Kalman filter solution ($\hat{\mathbf{x}}_{n|n}^e$) defined for the following system:

$$\mathbf{x}_{k+1}^e=\overbrace{(\mathbf{A}_k-\mathbf{N}_k(\mathbf{M}_k^3)^{-\mathbf{1}}\mathbf{T}_k^3\mathbf{C}_k)}^{\mathbf{A}_k^*}\mathbf{x}_k^e+\overbrace{\left|\mathbf{B}_k\quad -\mathbf{N}_k(\mathbf{M}_k^3)^{-\mathbf{1}}\right|\begin{vmatrix}\mathbf{w}_k\\ \mathbf{z}_k\end{vmatrix}}^{\mathbf{w}_k^*} \tag{20a}$$

$$\mathbf{y}_k^e=\underbrace{\mathbf{T}_k\mathbf{C}_k}_{\mathbf{C}_k^\#}\mathbf{x}_k^e+\mathbf{v}_k^1 \tag{20b}$$

$$E\left\{\begin{bmatrix}\mathbf{x}_0^e\\ \boldsymbol{\omega}_k\\ \mathbf{z}_k\\ \mathbf{v}_k^1\\ 1\end{bmatrix}\begin{bmatrix}\mathbf{x}_0^e\\ \boldsymbol{\omega}_k\\ \mathbf{z}_k\\ \mathbf{v}_k^1\end{bmatrix}^T\right\}=\begin{bmatrix}\mathbf{P}_0 & \mathbf{0} & \mathbf{0} & \mathbf{0}\\ \mathbf{0} & \mathbf{Q}_k & \mathbf{0} & \mathbf{0}\\ \mathbf{0} & \mathbf{0} & \overline{\mathbf{T}}_k\mathbf{R}_k\overline{\mathbf{T}}_k^T-\overline{\mathbf{T}}_k\mathbf{R}_k\mathbf{T}_k^T(\mathbf{T}_k\mathbf{R}_k\mathbf{T}_k^T)^{-1}\mathbf{T}_k\mathbf{R}_k\overline{\mathbf{T}}_k^T & \mathbf{0}\\ \mathbf{0} & \mathbf{0} & \mathbf{0} & \mathbf{T}_k\mathbf{R}_k\mathbf{T}_k^T\\ \mathbf{0} & \mathbf{0} & \mathbf{0} & \mathbf{0}\end{bmatrix} \tag{20c}$$

ii. The optimal $\hat{\mathbf{x}}_n$ is equal to

$$\hat{\mathbf{x}}_n=\mathbf{x}_n^N+\hat{\mathbf{x}}_n^e \tag{21}$$

where $\mathbf{x}_n^N$ is the state of the deterministic system defined in equation (18).

iii. The best $\mathbf{u}_n$ estimate is equal to $\hat{\mathbf{u}}_n=(\mathbf{M}_k^3)^{-1}(\mathbf{y}_k^3-\mathbf{T}_k^3\mathbf{C}_k\hat{\mathbf{x}}_n-\hat{\mathbf{z}}_n)$. The optimal $\hat{\mathbf{z}}_n$ is always zero because it is separate from the rest of the variables in equation (19) and it is not a part of the constraints at time n. Therefore,

$$\begin{aligned}\hat{\mathbf{u}}_n&=(\mathbf{M}_k^3)^{-1}(\mathbf{y}_k^3-\mathbf{T}_k^3\mathbf{C}_k\hat{\mathbf{x}}_n)\\&=(\mathbf{M}_k^3)^{-1}\mathbf{T}_k^3(\mathbf{y}_k-\mathbf{C}_k\hat{\mathbf{x}}_n).\end{aligned} \tag{22}$$

2.3. Implementation of the optimal solution

Lemma 2 might seem rather complicated. However, in this section, it will be shown that it is nothing more than what can be anticipated with the basic engineering intuition. To this end, we first prove that the term $(\mathbf{M}_k^3)^{-1}\mathbf{T}_k^3$ in Lemma 2 is in fact equivalent to the left (weighted) pseudo-inverse of the observations.

Property 1

When $\mathbf{R}_k$ is invertible, $(\mathbf{M}_k^3)^{-1}\mathbf{T}_k^3$ is equal to the weighted pseudo inverse of $\mathbf{M}_k$:

$$\begin{aligned}&(\mathbf{M}_k^3)^{-1}\mathbf{T}_k^3\\&\quad=(\overline{\mathbf{T}}_k\mathbf{M}_k)^{-1}(\overline{\mathbf{T}}_k-\overline{\mathbf{T}}_k\mathbf{R}_k\mathbf{T}_k^T(\mathbf{T}_k\mathbf{R}_k\mathbf{T}_k^T)^{-1}\mathbf{T}_k)\\&\quad=(\mathbf{M}_k^T\mathbf{R}_k^{-1}\mathbf{M}_k)^{-1}\mathbf{M}_k^T\mathbf{R}_k^{-1}\triangleq\mathbf{M}_k^*.\end{aligned} \tag{23}$$

Proof

Let $\mathbf{y}=\mathbf{M}\mathbf{x}+\mathbf{v}$, where $\mathbf{v}$ has a Gaussian $(\mathrm{N}(\mathbf{0},\mathbf{R}))$ distribution and $\mathbf{M}$ has full column rank. It is well known that the minimum variance estimate of $\mathbf{x}$ is $\hat{\mathbf{x}}^1=(\mathbf{M}^T\mathbf{R}^{-1}\mathbf{M})^{-1}\mathbf{M}^T\mathbf{R}^{-1}\mathbf{y}$.

Linear transformations on $\mathbf{y}$ do not change the optimal solution. Hence, the following two transformations can be applied on $\mathbf{y}$ without affecting the solution.

1. $\hat{\mathbf{T}}=\begin{vmatrix}\mathbf{T}\\ \overline{\mathbf{T}}\end{vmatrix}$ is a nonsingular matrix, where $\mathrm{Range}\{\overline{\mathbf{T}}^T\}=\mathrm{Range}\{\mathbf{M}\}$ and $\mathbf{TM}=\mathbf{0}$.

2. $\mathbf{V}=\begin{vmatrix}\mathbf{I} & \mathbf{0}\\ \underbrace{-\overline{\mathbf{T}}\mathbf{R}\mathbf{T}^T(\mathbf{T}\mathbf{R}\mathbf{T}^T)^{-1}}_{\tilde{\mathbf{T}}} & \mathbf{I}\end{vmatrix}$

Multiplying $\mathbf{V}\hat{\mathbf{T}}$ with $\mathbf{y}$, the following new sets of observations are obtained:

$$\begin{aligned}&\mathbf{T}\mathbf{y}=\mathbf{T}\mathbf{v}\\&(\overline{\mathbf{T}}-\tilde{\mathbf{T}}\mathbf{T})\mathbf{y}=\overline{\mathbf{T}}\mathbf{M}\mathbf{x}+(\overline{\mathbf{T}}-\tilde{\mathbf{T}}\mathbf{T})\mathbf{v}.\end{aligned} \tag{24}$$

$\overline{\mathbf{T}}\mathbf{M}$ is a full rank matrix by construction and $\mathbf{T}\mathbf{v}$ is orthogonal to $(\overline{\mathbf{T}}-\tilde{\mathbf{T}}\mathbf{T})\mathbf{v}$. Therefore, another optimal solution is $\hat{\mathbf{x}}^2=(\overline{\mathbf{T}}\mathbf{M})^{-1}(\overline{\mathbf{T}}-\tilde{\mathbf{T}}\mathbf{T})\mathbf{y}$.

The optimal solution is unique for this problem. Hence, $\hat{\mathbf{x}}^1=\hat{\mathbf{x}}^2$ for all $\mathbf{y}$. Therefore, $(\overline{\mathbf{T}}\mathbf{M})^{-1}(\overline{\mathbf{T}}-\tilde{\mathbf{T}}\mathbf{T})=(\mathbf{M}^T\mathbf{R}^{-1}\mathbf{M})^{-1}\mathbf{M}^T\mathbf{R}^{-1}=\mathbf{M}^*$, as stated in Property 1.

Using Property 1, the disturbance power in equation (20a) can be expressed as follows:

$$\begin{aligned}&E\{(\mathbf{N}_k(\mathbf{M}_k^3)^{-1}\mathbf{z}_k)(\mathbf{N}_k(\mathbf{M}_k^3)^{-1}\mathbf{z}_k)^T\}\\&\quad=\mathbf{N}_k(\mathbf{M}_k^3)^{-1}E\{\mathbf{z}_k\mathbf{z}_k^T\}(\mathbf{M}_k^3)^{-T}\mathbf{N}_k^T\\&\quad=\mathbf{N}_k(\mathbf{M}_k^3)^{-1}\mathbf{T}_k^3E\{\mathbf{v}_k\mathbf{v}_k^T\}\mathbf{T}_k^{3^T}(\mathbf{M}_k^3)^{-T}\mathbf{N}_k^T\\&\quad=\mathbf{N}_k\mathbf{M}_k^*E\{\mathbf{v}_k\mathbf{v}_k^T\}(\mathbf{N}_k\mathbf{M}_k^*)^T.\end{aligned} \tag{25}$$

After the application of Property 1 and equation (25) to Lemma 2, the final form of the optimization problem solution is obtained. This final form is summarized in the following lemma.

Lemma 3

1. The optimal $\mathbf{x}_n$ solution for the cost function defined in equation (7) is equal to

$$\hat{\mathbf{x}}_n=\mathbf{x}_n^N+\hat{\mathbf{x}}_n^e \tag{26}$$

where $\mathbf{x}_n^N$ is the state of the following deterministic system:

$$\begin{aligned}\mathbf{x}_{k+1}^N&=(\mathbf{A}_k-\mathbf{N}_k\mathbf{M}_k^*\mathbf{C}_k)\mathbf{x}_k^N+\mathbf{N}_k\mathbf{M}_k^*\mathbf{y}_k\\\mathbf{y}_k^N&=\mathbf{T}_k\mathbf{C}_k\mathbf{x}_k^N\\\mathbf{x}_0^N&=0\end{aligned} \tag{27}$$

and $\hat{\mathbf{x}}_n^e$ is the output of the Kalman filter defined for the following system

$$\mathbf{x}_{k+1}^{e} = \underbrace{(\mathbf{A}_k - \mathbf{N}_k\mathbf{M}_k^*\mathbf{C}_k)}_{\mathbf{A}_k^*}\mathbf{x}_k^e + \underbrace{\mathbf{B}_k\mathbf{w}_k - \mathbf{N}_k\mathbf{M}_k^*\mathbf{v}_k}_{\mathbf{w}_k^*} \quad (28a)$$

$$\underbrace{\mathbf{T}_k\mathbf{y}_k - \mathbf{y}_k^N}_{\mathbf{y}_k^e} = \underbrace{\mathbf{T}_k\mathbf{C}_k}_{\mathbf{C}_k^{\#}}\mathbf{x}_k^e + \mathbf{T}_k\mathbf{v}_k \quad (28b)$$

$$E\left\{\begin{bmatrix}\mathbf{x}_0^e\\ \mathbf{w}_k\\ \mathbf{v}_k\end{bmatrix}\begin{bmatrix}\mathbf{x}_0^e\\ \mathbf{w}_k\\ \mathbf{v}_k\end{bmatrix}^T\right\} = \begin{bmatrix}\mathbf{P}_0 & 0 & 0\\ 0 & \mathbf{Q}_k & 0\\ 0 & 0 & \mathbf{R}_k\end{bmatrix}, \quad \forall k. \quad (28c)$$

2. The optimal $\mathbf{u}_n$ for the cost function defined in equation (7) is equal to

$$\hat{\mathbf{u}}_n = \mathbf{M}_k^*(\mathbf{y}_n - \mathbf{C}_n\hat{\mathbf{x}}_n) \quad (29)$$

In equation (28) of Lemma 3, $\mathbf{T}_k\mathbf{v}_k$ is orthogonal to $\mathbf{N}_k\mathbf{M}_k^*\mathbf{v}_k$. Therefore, there is no cross-correlation between the observation and the system disturbance noise. Hence, any straightforward Kalman filter implementation can be used to compute $\hat{\mathbf{x}}_k^e$ and $\hat{\mathbf{x}}_k$. Such an implementation is presented in Figure 1. In this implementation, the pseudo inverse of the observations $(\mathbf{M}_k^*\mathbf{y}_k)$ is used to run the deterministic system that provides the nominal solution $\mathbf{x}_k^N$. The Kalman filter processes $\mathbf{T}_k\mathbf{y}_k$ to generate $\hat{\mathbf{x}}_k^e$, which is then added to $\mathbf{x}_k^N$ to obtain the optimal $\mathbf{x}_k$.

When $\mathbf{N}_k = 0$ in equation (5), the optimum solution takes a much simpler form. Under this condition, the output of the deterministic (nominal) part defined in equation (27) is always 0. Therefore, $\hat{\mathbf{x}}_k = \hat{\mathbf{x}}_k^e$, and the system model defined in equation (28) can be represented as follows:

$$\begin{aligned}\mathbf{x}_{k+1} &= \mathbf{A}_k\mathbf{x}_k + \mathbf{B}_k\mathbf{w}_k\\ \mathbf{T}_k\mathbf{y}_k &= \mathbf{T}_k\mathbf{C}_k\mathbf{x}_k + \mathbf{T}_k\mathbf{v}_k\end{aligned} \quad (30a)$$

$$E\left\{\begin{bmatrix}\mathbf{x}_0\\ \mathbf{w}_k\\ \mathbf{v}_k\end{bmatrix}\begin{bmatrix}\mathbf{x}_0\\ \mathbf{w}_k\\ \mathbf{v}_k\end{bmatrix}^T\right\} = \begin{bmatrix}\mathbf{P}_0 & 0 & 0\\ 0 & \mathbf{Q}_k & 0\\ 0 & 0 & \mathbf{R}_k\end{bmatrix}. \quad (30b)$$

An implementation of this form is presented in Figure 2. As can be seen from this figure, the optimal $\mathbf{u}_k$ values are obtained by computing the weighted average of the corrected sensor outputs $(\mathbf{y}_k - \mathbf{C}_k\hat{\mathbf{x}}_k)$.

3. Application to multi-inertial sensor fusion problem

In this section, based on the optimization structures described in the previous section, an optimal redundant inertial sensor fusion algorithm is derived.

3.1. Optimal sensor fusion algorithm for SRIMUs

The output of each inertial sensor in an SRIMU with N sensors can be represented as follows:

$${}^i\mathbf{x}_{k+1} = {}^i\mathbf{A}_k\,{}^i\mathbf{x}_k + {}^i\mathbf{B}_k\,{}^iw_k \quad (31a)$$

$${}^iy_k = {}^iC_k\mathbf{x}_k + {}^iv_k + {}^iM\mathbf{u}_k \quad (31b)$$

$$E\left\{\left|\begin{matrix}{}^i\mathbf{x}_0\\ {}^i\mathbf{w}_k\\ {}^iv_k\end{matrix}\right|\left|{}^i\mathbf{x}_0^T \quad {}^i\boldsymbol{\omega}_k^T \quad {}^iv_k^T\right|\right\} = \left|\begin{matrix}{}^i\mathbf{P}_0 & 0 & 0\\ 0 & {}^i\mathbf{Q}_k & 0\\ 0 & 0 & {}^iR_k\end{matrix}\right|, \quad \forall k \quad (31c)$$

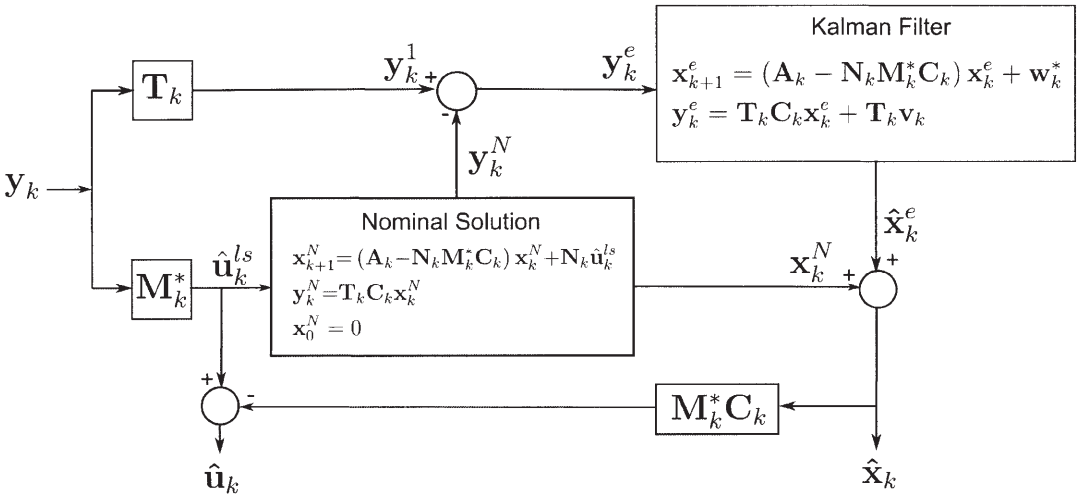

Figure 1: Structure for the optimal solution of the cost function defined in equation (7).

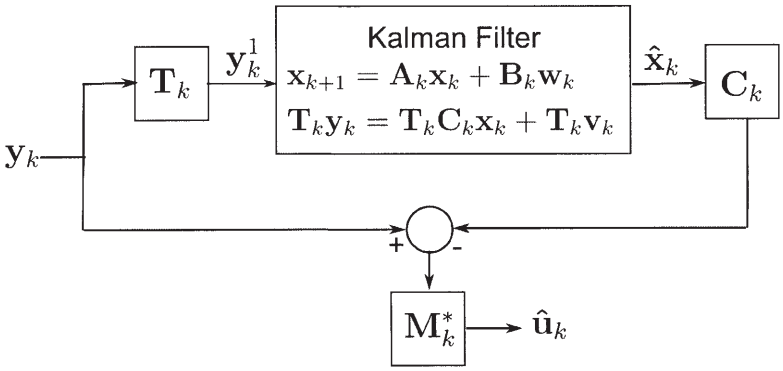

Figure 2: Optimal structure when $\mathbf{N}_k = 0$.

where each $\{{}^i y_k\}_{i=1}^N$ represents the individual (ith) sensor output, $\{{}^i\mathbf{x}_k\}_{i=1}^N$ is the corresponding sensor's error state, $\{{}^i v_k\}_{i=1}^N$ is the additive white noise component (i.e., ARV/VRW), $\{{}^i M_k\}_{i=1}^N$ is the unit vector in the direction of sensor's sensitive axis, and $\mathbf{u}_k$ is the real kinematic quantity that the sensors are expected to measure (i.e., acceleration/rotation rates). Both $\{{}^i C_k\}_{i=1}^N$ and $\{{}^i M_k\}_{i=1}^N$ are row vectors. $\{{}^i\mathbf{A}_k\}_{i=1}^N$ is the system matrix and $\{{}^i\mathbf{B}_k\}_{i=1}^N$ is a matrix with appropriate dimensions.

Combining all of the individual sensor representations into a single form, the following model for the entire SRIMU is obtained:

$$\mathbf{x}_{k+1} = \mathbf{A}_k\mathbf{x}_k + \mathbf{B}_k\mathbf{w}_k \tag{32a}$$

$$\mathbf{y}_k = \mathbf{C}_k\mathbf{x}_k + \mathbf{M}\mathbf{u}_k + \mathbf{v}_k \tag{32b}$$

$$E\{\mathbf{v}_k\mathbf{v}_k^T\} = \begin{bmatrix} {}^1R_k & 0 & 0 \\ 0 & \ddots & 0 \\ 0 & 0 & {}^N R_k \end{bmatrix} \triangleq \mathbf{R}_k \tag{32c}$$

where $\mathbf{y}_k = [{}^1 y_k; \quad \ldots \quad ; {}^N y_k]$ is the complete output vector of the SRIMU, $\mathbf{x}_k = [{}^1\mathbf{x}_k; \quad \ldots \quad ; {}^N\mathbf{x}_k]$ is the SRIMU state vector, $\mathbf{R}_k$ is the covariance matrix of the observation noise, and $\mathbf{M} = [{}^1 M; \quad \ldots \quad ; {}^N M]$ is the complete configuration matrix of the SRIMU. $\mathbf{A}_k$, $\mathbf{B}_k$, and $\mathbf{C}_k$ are formed by diagonally combining ${}^i\mathbf{A}_k$, ${}^i\mathbf{B}_k$, and ${}^i C_k$. Equation (32) is equal to equation (5) with $\mathbf{N}_k = 0$. Therefore, Lemma 3 (specifically Figure 2) can be directly used to compute the optimal acceleration/rotation rate ($\mathbf{u}_k$) estimate given all of the SRIMU outputs from time 0 to k. Based on Figure 2, the computation steps of this optimal sensor fusion algorithm are summarized in the following:

1. For each k, multiply the redundant sensor outputs with $\mathbf{T}_k$ to generate the observations to be processed by the Kalman filter. As shown in equation (10a), $\mathbf{T}_k$ is the basis for the left null space of the configuration matrix $\mathbf{M}$. The system model of the Kalman filter is as follows:

$$\begin{aligned} \mathbf{x}_{k+1} &= \mathbf{A}_k\mathbf{x}_k + \mathbf{B}_k\mathbf{w}_k \\ \mathbf{T}\mathbf{y}_k &= \mathbf{T}\mathbf{C}_k\mathbf{x}_k + \mathbf{T}\mathbf{v}_k \end{aligned} \tag{33}$$

2. Correct the raw sensor outputs with the Kalman filter outputs $\hat{\mathbf{x}}_k$.

3. Form the weighted average of the corrected outputs

$$\hat{\mathbf{u}}_k = \mathbf{M}^*(\mathbf{y}_k - \mathbf{C}_k\hat{\mathbf{x}}_k) \tag{34}$$

where

$$\mathbf{M}^* = (\mathbf{M}^T\mathbf{R}_k^{-1}\mathbf{M})^{-1}\mathbf{M}^T\mathbf{R}_k^{-1}. \tag{35}$$

The $\hat{\mathbf{u}}_k$ computed with these steps corresponds to the optimal solution of the cost function defined in equation (7).

In addition to this result, it is also necessary to derive an error model for the optimal $\hat{\mathbf{u}}_k$ values. Such error models are required in the navigation Kalman filters when the INSs are integrated with the external aids.

Let $\mathbf{e}_k = \hat{\mathbf{u}}_k - \mathbf{u}_k$ be the error on the optimally fused SRIMU output. Then,

$$\begin{aligned} \mathbf{e}_k &= \mathbf{M}^*(\mathbf{y}_k - \mathbf{C}_k\hat{\mathbf{x}}_k) - \mathbf{u}_k \\ &= \mathbf{M}^*(\mathbf{C}_k(\mathbf{x}_k - \hat{\mathbf{x}}_k) + \mathbf{M}\mathbf{u}_k + \mathbf{v}_k) - \mathbf{u}_k \\ &= \mathbf{M}^*\mathbf{C}_k\tilde{\mathbf{x}}_k + \mathbf{M}^*\mathbf{v}_k \end{aligned} \tag{36}$$

where $\tilde{\mathbf{x}}_k$ represents the error on the filtered output ($\hat{\mathbf{x}}_k$) of the Kalman filter:

$$\begin{aligned} \tilde{\mathbf{x}}_k &= \mathbf{x}_k - \hat{\mathbf{x}}_k \\ &= (\mathbf{I} - \mathbf{K}_k\mathbf{T}\mathbf{C}_k)\mathbf{A}_{k-1}\tilde{\mathbf{x}}_{k-1} \\ &\quad + (\mathbf{I} - \mathbf{K}_k\mathbf{T}\mathbf{C}_k)\mathbf{B}_{k-1}w_{k-1} - \mathbf{K}_k\mathbf{T}\mathbf{v}_k \end{aligned} \tag{37}$$

In equation (37), $\mathbf{K}_k$ is the gain of Kalman filter used for the system defined in equation (33).

3.2. Optimal sensor fusion algorithm for identical inertial units

When all of the inertial sensors in an SRIMU have identical stochastic error models, the simple weighted average of the raw sensor outputs becomes the optimal solution (i.e., $\hat{\mathbf{u}}_k = \mathbf{M}^*\mathbf{y}_k$). In other words, under these conditions, the upper branch in Figure 2 (i.e., the Kalman filter) is not needed. Furthermore, the number of states in the final error models defined in equations (36) and (37) can be significantly reduced. In this section, such properties of SRIMUs with identical sensors are analyzed.

As can be seen from Figure 2, the optimal $\hat{\mathbf{u}}_k$ value is only affected by a certain combination (i.e., $\mathbf{M}^*\mathbf{C}_k\mathbf{x}_k$) of the sensor error states. In the following, it is proved that this combination of states becomes orthogonal to the observations ($\mathbf{T}\mathbf{y}_k$) when the sensors have identical yet independent error models.

The cross-covariance between the observations and required combination of states can be represented as follows:

$$E\{\mathbf{M}^*\mathbf{C}_k\mathbf{x}_k\mathbf{y}_l^T T^T\} = \mathbf{M}^*\mathbf{C}_k \underbrace{E\{\mathbf{x}_k\mathbf{x}_l^T\}}_{\mathbf{P}_{kl}} \mathbf{C}_k^T\mathbf{T}^T. \quad (38)$$

Assuming there exist N sensors, $\mathbf{P}_{kl} = diag({}^1\mathbf{P}_{kl} \ \ldots \ {}^N\mathbf{P}_{kl})$ is itself a block diagonal matrix with identical block diagonal elements. Therefore,

$$\mathbf{C}_k\mathbf{P}_{kl}\mathbf{C}_l^T = \gamma_{kl}\mathbf{I} \quad (39)$$

where γ_{kl} is a scalar. Using equation (39) in equation (38), the following result is obtained:

$$\begin{aligned}\mathbf{M}^*\mathbf{C}_k\mathbf{P}_{kl}\mathbf{C}_k^T\mathbf{T}^T &= \gamma_{kl}\mathbf{M}^*\mathbf{T}^T \\ &= \gamma_{kl}(\mathbf{M}^T\mathbf{R}_k^{-1}\mathbf{M})^{-1}\mathbf{M}^T\mathbf{R}_k^{-1}\mathbf{T}^T \\ &= \gamma_{kl}(\mathbf{M}^T\mathbf{M})^{-1}\underbrace{(\mathbf{T}\mathbf{M})}_{0}{}^T = 0. \end{aligned} \quad (40)$$

This shows that observations are always orthogonal to the required combination of states under the specified conditions. This orthogonality implies that $\mathbf{M}^*\mathbf{C}_k\hat{\mathbf{x}}_k = 0$ for all k. Therefore, the optimal $\mathbf{u}_k$ value is equal to $\hat{\mathbf{u}}_k = \mathbf{M}^*\mathbf{y}_k - \mathbf{M}^*\mathbf{C}_k\hat{\mathbf{x}}_k = \mathbf{M}^*\mathbf{y}_k$ as claimed earlier.

Under these conditions, the error model of the optimal output $\hat{\mathbf{u}}_k$ also has a relatively simple form as shown in the following:

Let $\mathbf{e}_k = \hat{\mathbf{u}}_k - \mathbf{u}_k$, then:

$$\begin{aligned}\mathbf{e}_k &= \mathbf{M}^*\mathbf{y}_k - \mathbf{u}_k \\ &= \mathbf{M}^*(\mathbf{M}\mathbf{u}_k + \mathbf{C}_k\mathbf{x}_k + \mathbf{v}_k) - \mathbf{u}_k \\ &= \mathbf{M}^*\mathbf{C}_k\mathbf{x}_k + \mathbf{M}^*\mathbf{v}_k \end{aligned} \quad (41)$$

where the model of $\mathbf{x}_k$ is defined in equation (32a). The correlation structure of $\mathbf{e}_k$ can be represented as:

$$\begin{aligned}E\{\mathbf{e}_k\mathbf{e}_l^T\} &= E\{(\mathbf{M}^*\mathbf{C}_k\mathbf{x}_k + \mathbf{M}^*\mathbf{v}_k) \\ &\quad \times (\mathbf{M}^*\mathbf{C}_k\mathbf{x}_k + \mathbf{M}^*\mathbf{v}_k)^T\} \\ &= \mathbf{M}^*\underbrace{\mathbf{C}_k E\{\mathbf{x}_k\mathbf{x}_l^T\}\mathbf{C}_k^T}_{\gamma_{kl}\mathbf{I}}\mathbf{M}^{*T} \\ &\quad + \mathbf{M}^*\underbrace{E\{\mathbf{v}_k\mathbf{v}_l^T\}}_{R_k\mathbf{I}\delta[k-l]}\mathbf{M}^{*T} \\ &= \gamma_{kl}(\mathbf{M}^T\mathbf{M})^{-1} + R_k(\mathbf{M}^T\mathbf{M})^{-1}\delta[k-l] \\ &= (\gamma_{kl} + R_k\delta[k-l])(\mathbf{M}^T\mathbf{M})^{-1}. \end{aligned} \quad (42)$$

If an SRIMU contains N sensors and each sensor is modeled with M states, the model of $\mathbf{e}_k$ theoretically requires $N*M$ states. However, as the Kalman filters use only second-order stochastic properties, any model with a lower number of states can also be used in the navigation Kalman filters, so long as the alternative model has exactly the same correlation structure defined in equation (42). In Figure 3, such an alternative model for $\mathbf{e}_k$ is presented. This model assumes that the SRIMU contains only one sensor per axis, which has the same error characteristics as any one of the real sensors. Therefore, assuming the SRIMU spans all three kinematic axes, only $3*M$ states are required to model the error $\mathbf{e}_k$ in this structure.

4. Simulation results

4.1. Example I

A simulation result showing the optimum solution of the system introduced in Section 1.1 is presented in this example. As described in Section 1.1, this conceptual system contains two gyroscopes that are used to sense the rotation of the wheel. The sensitive axes of both gyroscopes are parallel to the axis of rotation of the wheel. The redundant sensors' output model is defined in equation (1). It was assumed that the true rotation rate of the wheel with respect to inertial space is

$$\omega(t) = 0.0014\sin\left(\frac{2\pi}{12}t\right) \quad {}^\circ/\text{sec}. \quad (43a)$$

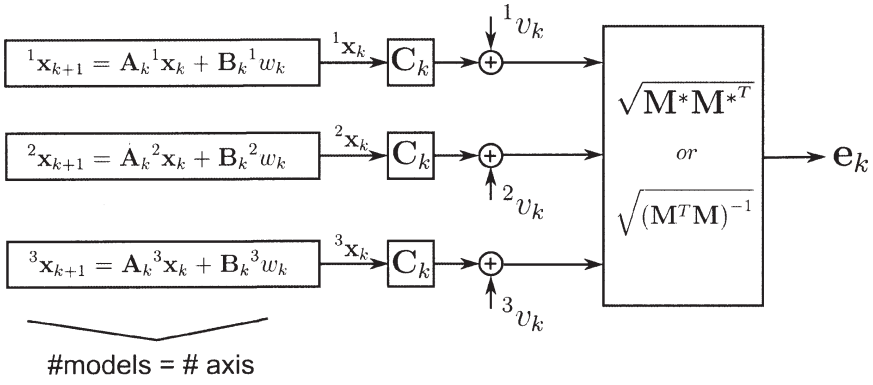

Figure 3: Alternative model for $\mathbf{e}_k$ when the SRIMU spans all three kinematic axes. The model parameters for each axis (i.e., $\mathbf{A}_k$, $\mathbf{B}_k$, $\mathbf{w}_k$, v_k) are the same as the real one. The autocorrelation of $\mathbf{e}_k$ is equal to the autocorrelation defined in equation (42).

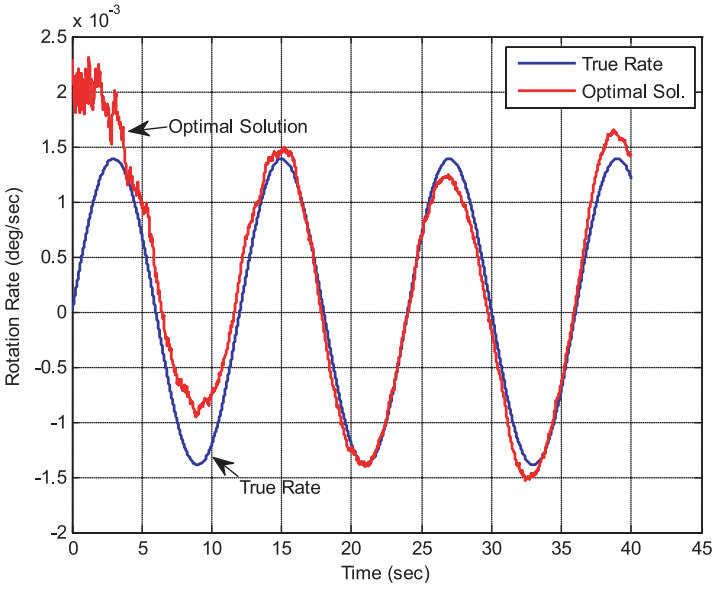

Figure 4: Comparison of true rotation rate and optimally fused gyroscope outputs.

The following values are used in equation (1c) during the simulations at 100 Hz:

$$R = 1^{-4}, \quad P = 1^{-6}, \quad Q = 1.6^{-11} \quad (^\circ/\text{sec})^2. \quad \text{(43b)}$$

Based on these values, 40 s of gyroscope data was simulated for both sensors. Then, the generated data set was processed to compute the optimally fused outputs using the structure shown in Figure 2. The comparison of the true rotation rate with the optimally fused outputs is presented in Figure 4. As seen from this figure, after a transient period, the error on the optimally fused outputs decreased significantly.

The rotation angle of the wheel can be computed by integrating the optimally fused gyroscope outputs as shown in equation (2). However, the angle obtained in this way is not the optimal angle solution. To compute the optimal angle estimate, the problem should be formulated with the angle state as a part of the overall system model as shown in the following:

$$\underbrace{\begin{bmatrix} x^a_{k+1} \\ x^1_{k+1} \end{bmatrix}}_{\mathbf{x}_{k+1}} = \underbrace{\begin{bmatrix} 1 & 0 \\ 0 & 1 \end{bmatrix}}_{\mathbf{A}} \underbrace{\begin{bmatrix} x^a_k \\ x^1_k \end{bmatrix}}_{\mathbf{x}_k} + \underbrace{\begin{bmatrix} \Delta t \\ 0 \end{bmatrix}}_{\mathbf{N}} \omega_k + \underbrace{\begin{bmatrix} 0 \\ w^1_k \end{bmatrix}}_{\mathbf{w}_k} \quad \text{(44a)}$$

$$\underbrace{\begin{bmatrix} y^1_k \\ y^2_k \end{bmatrix}}_{\mathbf{y}_k} = \underbrace{\begin{bmatrix} 1 \\ 1 \end{bmatrix}}_{\mathbf{M}} \omega_k + \underbrace{\begin{bmatrix} x^1_k \\ 0 \end{bmatrix}}_{\mathbf{x}_k} + \underbrace{\begin{bmatrix} 0 \\ v^2_k \end{bmatrix}}_{\mathbf{v}_k} \quad \text{(44b)}$$

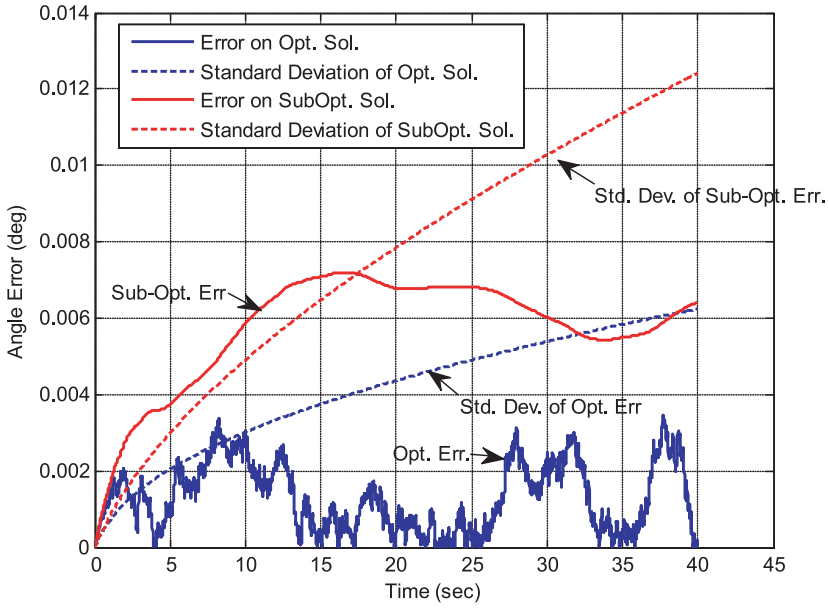

Figure 5: Comparison of computed angle errors for optimal and suboptimal methods.

where all parameters are defined in equations (1) and (2). This formulation has exactly the same form with equation (5). Therefore, the general solution defined in Lemma 3 (Figure 1) can be applied to compute the optimal angle estimate.

In Figure 5, the comparison of this optimal angle estimate with the angle computed by integrating the optimally fused sensor outputs is presented. As can be seen from this figure, the error (and the standard deviation of the error) on the optimal angle solution is less than the other solution.

This example hints at the fact that when an INS is run only by optimally fused sensor outputs, the navigation results cannot be regarded as optimal. In general, the optimal navigation result requires the sensor redundancy measurements to be processed by the navigation Kalman filter as shown by Pittelkau (2005a) and Allerton and Jia (2007). However, we observed in extensive simulation studies that the difference between the optimal and the above type of suboptimal solutions can be regarded as marginal and, hence, can be ignored in favor of ease of implementation for almost all realistic scenarios.

The relation between the optimal and suboptimal navigation solutions for the SRIMU-based INSs is beyond the content of this study. Therefore, this point will not be pursued any further. Interested readers can refer to the work of Yuksel (2011) for a detailed analysis of such relations. The focus of the remaining examples will be confined to the optimal sensor fusion results.

4.2. Example II

In this example, the same system described in Section 1.1 was simulated under different sensor error characteristics. The complete sensor observation model and the new sensor error models used in this simulation are as follows:

$$\underbrace{\begin{bmatrix} y_k^1 \\ y_k^2 \end{bmatrix}}_{\mathbf{y}_k} = \underbrace{\begin{bmatrix} 1 \\ 1 \end{bmatrix}}_{\mathbf{M}} \underbrace{\omega_k}_{u_k} + \underbrace{\begin{bmatrix} x_k^1 \\ x_k^2 \end{bmatrix}}_{\mathbf{x}_k} + \underbrace{\begin{bmatrix} {}^1v_k \\ {}^2v_k \end{bmatrix}}_{\mathbf{v}_k} \tag{45a}$$

$$\begin{bmatrix} x_{k+1}^1 \\ x_{k+1}^2 \end{bmatrix} = \underbrace{\begin{bmatrix} 0.995 & 0 \\ 0 & 0.998 \end{bmatrix}}_{\mathbf{A}} \underbrace{\begin{bmatrix} x_k^1 \\ x_k^2 \end{bmatrix}}_{\mathbf{x}_k} + \underbrace{\begin{bmatrix} w_k^1 \\ w_k^2 \end{bmatrix}}_{\mathbf{w}_k} \tag{45b}$$

$$E\{\mathbf{v}_k\mathbf{v}_k^T\} = \mathbf{R} = \begin{bmatrix} 2.5^{-5} & 0 \\ 0 & 5.5^{-4} \end{bmatrix} \tag{45c}$$

$$E\{\mathbf{w}_k\mathbf{w}_k^T\} = \begin{bmatrix} 7.5^{-5} & 0 \\ 0 & 2^{-5} \end{bmatrix} \tag{45d}$$

where y_k^1 and y_k^2 represents the gyroscope 1 and 2 outputs, respectively, x_k^1 and x_k^2 are the stability error states of the corresponding gyroscopes, and ω_k is the true rotation rate, which was generated

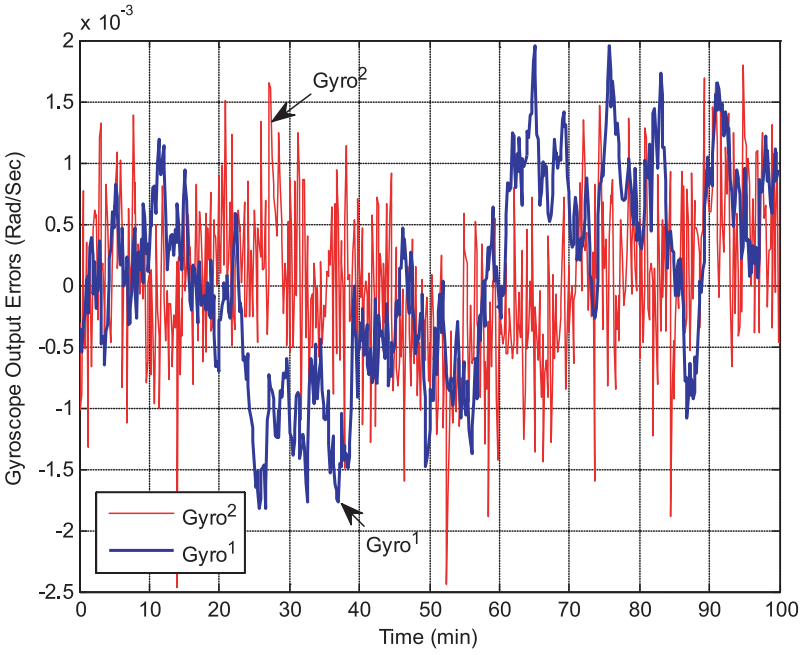

Figure 6: Comparison of simulated gyroscope output errors.

using the Matlab "rand( )" command during the simulations to emphasize the independence of the errors to the simulated inputs. As can be seen in equations (36) and (37), the error on the optimally fused outputs does not depend on the real kinematic variables.

The simulated raw gyroscope output errors ($y_k^1 - \omega_k$, $y_k^2 - \omega_k$) are presented in Figure 6. As can be seen from this figure, these two gyroscopes have complimentary characteristics. Although gyroscope 2 has better stability characteristics, it suffers from the additive white noise errors more than the gyroscope 1. Two types of fusion algorithms were implemented to generate a single, combined rotation rate measurement from these simulated gyroscope outputs. The first one is the optimal sensor fusion algorithm, which is described in Lemma 3 (Figure 2). The second algorithm is the simple weighted average of both sensors where $\mathbf{R}$ in equation (45c) was used as the weight matrix. The errors on the outputs of these two algorithms are compared in Figure 7. As can be seen from this figure, the error on the weighted average solution is almost identical to the error on the raw gyroscope 1 output. On the other hand, the error on the optimal solution inherits its stability characteristics from gyroscope 2 and its white noise characteristics from gyroscope 1. This figure suggests that the optimal solution has the property of blending the best characteristics of individual sensors, which is a clear advantage over the weighted-average-type solutions when the sensors have different (but complimentary) characteristics.

4.3. *Example III*

In this example, a 2DoF skew-redundant accelerometer unit with six identical sensors was simulated. The orientation of the sensitive axis of each accelerometer in this SRIMU is presented in Figure 8. It should be noted that this configuration is one of two configurations that minimize the geometric dilution of precision measure defined by Sturza (1988).

The output model of the accelerometers ($\{\mathrm{Acc}^i\}_{i=0}^5$) that are simulated in this example is as follows:

$$ {}^i y_k = {}^i M \underbrace{\begin{bmatrix} a_k^x \\ a_k^y \end{bmatrix}}_{\mathbf{u}_k} + [1 \quad 1] \underbrace{\begin{bmatrix} {}^i x_k^s \\ {}^i x_k^b \end{bmatrix}}_{{}^i x_k} + {}^i v(k) \tag{46a} $$

$$ \underbrace{\begin{bmatrix} {}^i x_{k+1}^s \\ {}^i x_{k+1}^b \end{bmatrix}}_{{}^i x_{k+1}} = \underbrace{\begin{bmatrix} 0.9987 & 0 \\ 0 & 1 \end{bmatrix}}_{{}^i \mathbf{A}_k} \begin{bmatrix} {}^i x_k^s \\ {}^i x_k^b \end{bmatrix} + \underbrace{\begin{bmatrix} {}^i w_k^1 \\ {}^i w_k^2 \end{bmatrix}}_{{}^i \mathbf{w}_k} \tag{46b} $$

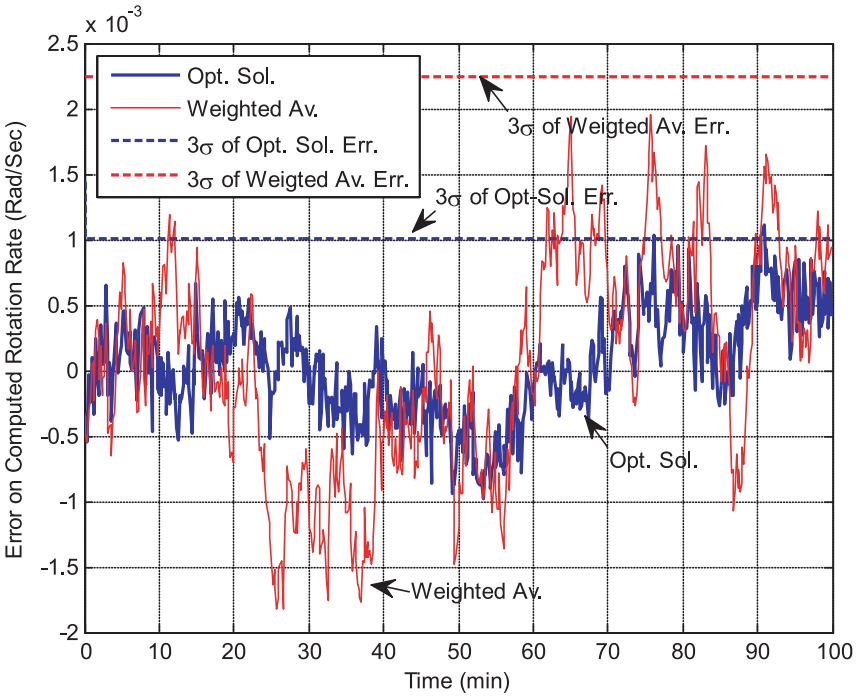

Figure 7: Comparison of errors on the computed rotation rates. Dashed lines represent 3∗standard deviations of the corresponding errors.

$$E\left\{\begin{bmatrix} {}^{i}x_0 \\ {}^{i}\mathbf{w}_k \\ {}^{i}v_k \end{bmatrix}\begin{bmatrix} {}^{i}x_0 \\ {}^{i}\mathbf{w}_k \\ {}^{i}v_k \end{bmatrix}^T\right\}$$

$$= \begin{bmatrix} \underbrace{\begin{bmatrix} 4.7^{-7} & 0 \\ 0 & 3.6^{-5} \end{bmatrix}}_{{}^{i}\mathbf{P}_0} & 0 & 0 \\ 0 & \underbrace{\begin{bmatrix} 0.1223^{-8} & 0 \\ 0 & 0 \end{bmatrix}}_{{}^{i}\mathbf{Q}} & 0 \\ 0 & 0 & \underbrace{0.85^{-8}}_{{}^{i}R} \end{bmatrix} \quad (46c)$$

$${}^{i}M = [\cos(i^*\pi/3) \quad \sin(i^*\pi/3)] \quad (46d)$$

where ${}^{i}y_k$ represents the Acc^{i} output, ${}^{i}x_k$ is the error state of the accelerometer, which consists of a stability (${}^{i}x_k^s$) and a repeatability (${}^{i}x_k^b$) part, ${}^{i}M$ is the unit vector in the direction of the sensitive axis, and a_k^x and a_k^y are the real acceleration values on the x and y axes, respectively. These error model parameters were obtained as a result of a laboratory modeling test performed on an LIS3L02AL (STMicroelectronics 2006) unit.

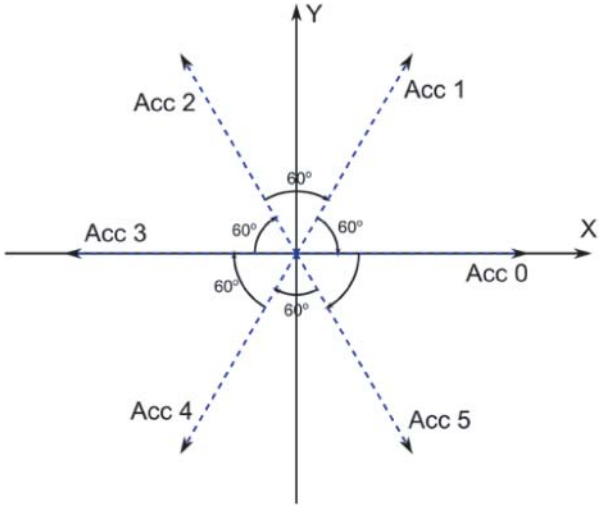

Figure 8: Accelerometer orientations. Each dashed line represents the sensitive axis of an accelerometer in the 2DoF SRIMU block.

Based on the individual error models defined in equation (46), the overall output model of the SRIMU can be written in a compact form as follows:

$$\underbrace{\begin{bmatrix} {}^0y_k \\ \vdots \\ {}^5y_k \end{bmatrix}}_{\mathbf{y}_k} = \underbrace{\begin{bmatrix} {}^0M \\ \vdots \\ {}^5M \end{bmatrix}}_{\mathbf{M}} \underbrace{\begin{bmatrix} a_k^x \\ a_k^y \end{bmatrix}}_{\mathbf{u}_k} + \underbrace{\begin{bmatrix} [1 \quad 1] & 0 & 0 \\ 0 & \ddots & 0 \\ 0 & 0 & [1 \quad 1] \end{bmatrix}}_{C} \underbrace{\begin{bmatrix} {}^0x_k \\ \vdots \\ {}^5x_k \end{bmatrix}}_{\mathbf{x}_k} + \underbrace{\begin{bmatrix} {}^0v_k \\ \vdots \\ {}^5v_k \end{bmatrix}}_{\mathbf{v}_k}. \tag{47}$$

For this SRIMU configuration and the error model parameters, a 10-min data set was simulated. The generated data set was then processed using the two following methods to compute a combined acceleration measurement $\hat{\mathbf{u}}_k$ for each k.

1. Weighted-average solution: This solution was computed as follows:

$$\hat{\mathbf{u}}_k^{\text{wa}} = (\mathbf{M}^T\mathbf{R}^{-1}\mathbf{M})^T\mathbf{M}^T\mathbf{R}^{-1}\mathbf{y}_k$$

   where $\mathbf{R} = E\{\mathbf{v}_k\mathbf{v}_k^T\}$.
2. Optimal solution: This was computed as described in Lemma 3 (Figure 2).

The errors on the computed x and y accelerations are presented in Figure 9 for these two types of solutions. As seen from this figure, the errors on the optimal and weighted-average solutions are exactly the same. This is an anticipated result because when all the sensors are identical, the redundancy observations become orthogonal to the kinematic variable estimates (the acceleration values). Therefore, as described in Section 3.2, the Kalman filter in the optimal solution becomes functionless and the two types of solution become identical.

In Section 3.2, it is shown that when all the sensors in an SRIMU have identical error models, the error on $\hat{\mathbf{u}}_k$ can be modeled with a lower number of states using the structure presented in Figure 4. For this example, such a reduced-order error model is presented in the following.

Let $\mathbf{e}_k = \hat{\mathbf{u}}_k - \mathbf{u}_k$ be the error on the computed accelerations. The autocorrelation of $\mathbf{e}_k$ is equal to the autocorrelation of the following model output:

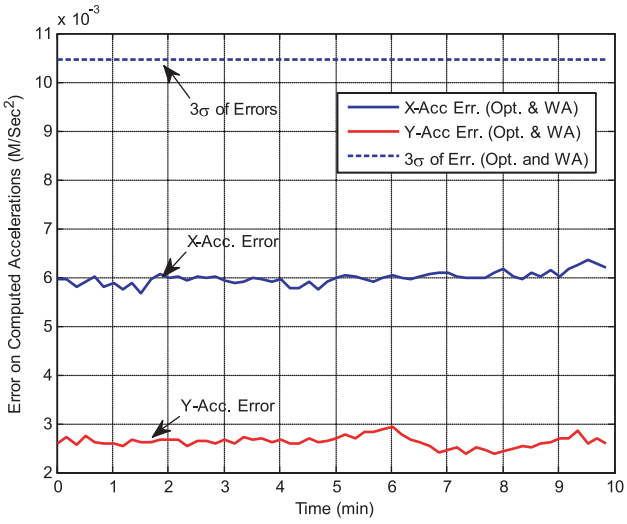

Figure 9: Errors on the acceleration values computed using optimal and weighted-average solutions. As the errors are identical for each type of solution, the corresponding error curves seem as a single curve. Dashed line represents the 3∗standard deviation of the errors for both optimal and weighted-average solutions on both x and y axes.

$$\mathbf{e}_k = \sqrt{(\mathbf{M}^T\mathbf{M})^{-1}} \left(\begin{bmatrix} [1 \quad 1] & [0 \quad 0] \\ [0 \quad 0] & [1 \quad 1] \end{bmatrix} \begin{bmatrix} {}^0x_k^s \\ {}^0x_k^b \\ {}^1x_k^s \\ {}^1x_k^b \end{bmatrix} + \begin{bmatrix} {}^0v(k) \\ {}^1v(k) \end{bmatrix} \right) \tag{48}$$

where $\mathbf{M}$ is the configuration matrix of the SRIMU and $\{{}^ix_k^b, {}^ix_k^s, {}^iv_k\}_{i=0}^1$ are exactly as defined in equation (46). It should be noted that only four states are used to represent the errors on the computed acceleration values in this reduced-order model, whereas a true model requires 12 states. Such model reductions provide tremendous flexibility when tens of identical sensors are used in an SRIMU.

5. Conclusions and discussion

In this study, an optimal sensor fusion algorithm was described for the SRIMUs. The optimality of the solution is defined based on a deterministic quadratic cost function. Although there are similar algorithms in the existing literature, the new framework that has been introduced in this study to define the optimality has never been published before.

Some key points and the limitations of this study are summarized here:

1. In this study, the optimal solution is defined based on a deterministic cost function. Therefore, even with partial knowledge of inertial sensors' error models, the algorithm can still be applied.
2. As seen in equation (5), the cost function does not depend on the configuration matrix. This means that the solution is not globally optimal. The optimality claim is valid under the predefined (given) sensor configuration.
3. The usefulness of the optimal fusion algorithm is directly related to the characteristics of the individual sensors. If the sensors have identical error models, the simple weighted-average solution becomes the optimal solution. Therefore, unless the sensors have complimentary characteristics, the proposed fusion algorithm will not provide any noticeable improvement over weighted-average solutions.

References

Allerton, D. J. and Jia, H., "An error compensation method for skewed redundant inertial configuration," Proceedings of the 58th Annual Meeting of the Institute of Navigation and CIGTF 21st Guidance Test Symposium, Albuquerque, NM, June 2002, pp. 142–147.

Allerton, D. J. and Jia, H., "Redundant multi-mode filter for a navigation system," IEEE Transactions on Aerospace and Electronic Systems, vol. 43, no. 1, pp. 371–391, January 2007.

Bar-Itzhack, I. Y. and Harman, R. R., "In-space calibration of a skewed gyro quadruplet," Journal of Guidance, Control, and Dynamics, vol. 25, no. 5, pp. 852–859, 2002.

Bejczy, A. K., "Non-orthogonal redundant configurations of single-axis struppedown gyros," JPL Quarterly Technical Review, vol. 1, no. 2, pp. 107–118, July 1971.

Basseville, M., "Information criteria for residual generation and fault detection and isolation," Inria Research Report, RR-2890, 1996.

Chen, T.-T. and Adams, M., "A sequential failure detection technique and its application," IEEE Transactions on Automatic Control, vol. 21, no. 5, pp. 750–757, October 1976.

Chow, E. and Willsky, A., "Analytical redundancy and the design of robust failure detection systems," IEEE Transactions on Automatic Control, vol. 29, no. 7, pp. 603–614, July 1984.

Daly, K. C., Gai, E. and Harrison, J. V., "Generalized likelihood test for FDI in redundant sensor configurations," Journal of Guidance and Control, vol. 2, no. 1, pp. 9–17, 1979.

DeAngelis, F. E., "A threshold redundancy management algorithm for skewed sensor arrays," Proceedings of the IEEE/AIAA/NASA 9th Digital Avionics Systems Conference, October 15–18, 1990, pp. 133–140.

Deckert, J., Desai, M., Deyst, J. and Willsky, A., "F-8 DFBW sensor failure identification using analytic redundancy," IEEE Transactions on Automatic Control, vol. 22, no. 5, pp. 795–803, October 1977.

Desai, M. and Ray, A., "A fault detection and isolation methodology," 20th IEEE Conference on Decision and Control, including the Symposium on Adaptive Processes, December 1981, vol. 20, pp. 1363–1369.

Evans, F. A. and Wilcox, J. C., "Experimental strapdown redundant sensor inertial navigation system," Journal of Spacecraft and Rockets, 0022-4650, vol. 7, no. 9, pp. 1070–1074, 1970.

Frank, P. M., "Fault diagnosis in dynamic system using analytical and knowledge based redundancy – a survey and some new results," Automatica, vol. 26, no. 3, 459–474, 1990.

Hall, S. R., "Parity vector compensation for FDI," MS thesis, Department of Aeronautics and Astronautics, Massachusetts Institute of Technology, Cambridge, MA, February 1982.

Harrison, J. V. and Gai, E. G., "Evaluating sensor orientations for navigation performance and failure detection," IEEE Transactions on Aerospace and Electronic Systems, vol. AES-13, no. 6, pp. 631–643, November 1977.

Hassibi, B., Sayed, A. H. and Kailath, T., Indefinite-Quadratic Estimation and Control: A Unified Approach to H2 and H-Infinity Theories, Studies in Applied and Numerical Mathematics, vol. 16, SIAM, Philadelphia, PA, 1999.

Ho, J. H., "Sensor redundancy management/fault detection and isolation of the inertial measurement unit for a land-based vehicle's locating system," PhD dissertation, Department of Mechanical Engineering, Pennsylvania State University, University Park, PA, October 1999.

Jia, H., "Data fusion methodologies for multisensor aircraft navigation systems," PhD dissertation, Cranfield University, Bedfordshire, UK, 2004.

Kerr, T., "Decentralized filtering and redundancy management for multisensor navigation," IEEE Transactions on Aerospace and Electronic Systems, vol. AES-23, no. 1, pp. 83–119, January 1987.

Patton, R. J. and Ghent, J., "Review of parity space approaches to fault diagnosis for aerospace systems," Journal of Guidance Control and Dynamics, vol. 17, no. 2, pp. 278–285, March–April 1994.

Patton, R. J., Frank, P. M. and Clark, R. N., Issues of Fault Diagnosis for Dynamic Systems, Springer-Verlag, London, 2000.

Pejsa, A. J., "Optimum skewed redundant inertial navigators," AIAA Journal, vol. 12, no. 7, pp. 899–902, 1974.

Pittelkau, M. E., "Calibration and attitude determination with redundant inertial measurement units," AIAA Journal of Guidance, Control, and Dynamics, vol. 28, no. 4, pp. 743–752, July–August 2005a.

Pittelkau, M. E., "Observability and calibration of a redundant inertial measurement unit (RIMU)", AAS 05-105, AAS/AIAA Space Flight Mechanics Meeting, Copper Mountain, CO, January 23–27, 2005, In Advances in the Astronautical Sciences, Vol. 120, Part I, 2005, pp. 71–84, 2005b.

Pittelkau, M. E., "Cascaded and decoupled RIMU calibration filters," Paper AAS 05-466, Malcom D. Shuster Astronautics Symposium, Grand Island, NY, June 12–15, 2005, In Advances in the Astronautical Sciences, vol. 122, pt. I, pp. 273–288, 2006.

Ray, A., "Sequential testing for fault detection in multiply-redundant systems," ASME Journal of Dynamic Systems, Measurement, and Control, vol. 111, no. 2, pp, 329–332, 1989.

Sukkarieh, S., Gibbens, P., Grocholsky, B., Willis, K. and Durrant-Whyte, H. F., "A low-cost, redundant inertial measurement unit for unmanned air vehicles," International Journal of Robotics Research, vol. 19, no. 11, pp. 1089–1103, November 2000.

Skoogh, D. and Lennartsson, A., "A method for multiple fault detection and isolation of redundant inertial navigation sensor configurations," Proceedings of IEEE/ION PLANS 2006, San Diego, CA, April 2006, pp. 415–425.

STMicroelectronics LIS3L02AL MEMS Inertial Sensor 3-Axis Ultracompact Linear Accelerometer Data Sheet, STMicroelectronics, La Jolla, CA, 2006.

Sturza, M. A., "Skewed axis inertial sensor geometry for optimal performance," 8th AIAA/IEEE Digital Avionics Systems Conference, Technical Papers, Part 1, A89-18051 05–06, October 1988, pp. 128–135.

Wilcox, J. C., Competitive Evaluation of Failure Detection Algorithms for Strapdown Redundant Inertial Instruments—Final Report, TRW Report 18313-6004, TRW Systems Groups, Redondo Beach, CA, USA, 1973.

Yuksel, Y., "Design and analysis of inertial navigation systems with skew redundant inertial sensors," PhD thesis, Department of Geomatics Engineering, University of Calgary, Calgary, Alberta, Canada, 2011.

Yuksel, Y., El-Sheimy, N. and Aboelmagd, N., "Error modeling and characterization of environmental effects for low cost inertial MEMS units," Position Location and Navigation Symposium (PLANS), May 4–6, 2010, IEEE/ION, pp. 598–612, 2010.

Author information
Department of Geomatics Engineering
University of Calgary
Calgary, Alberta, Canada
E-mail: yyuksel@ucalgary.ca